Chemo-kinematic characterisation of the Red Clump stars of the Galactic bar

Author: Jordi Mangues Estany.
Facultat de Física, Universitat de Barcelona, Diagonal 645, 08028 Barcelona, Spain.

Advisor: Mercè Romero-Gómez
Departament de Física Quàntica i Astrofísica

Abstract: Thanks to recent surveys, we now have larger homogeneous data sets containing kinematics and metallicities of stars outside the solar neighbourhood. From a cross-match between Gaia DR2 and APOGEE DR16 data, we can study the complex chemical and dynamical structure of the galactic disk, which is perturbed by the existence of a galactic bar. We run an orbital integrator to classify the 3D quasiperiodic orbits into the different resonant families. Since the cross-match between GAIA DR2 and APOGEE DR16 data gives us also the metallicities, we then investigate the effect of bar resonances on the metallicity distribution in the Milky Way.

I. INTRODUCTION

The Milky Way is a spiral barred galaxy. The data realeased by GAIA DR2, revealed that the galactic disk is dynamically more complex than it was thought to be [e.g., 4, 7, 10]. There are many perturbers at play, which specific influence is still not clear, the spiral structure, galactic bar and satellite galaxies are all examples of perturbers that play an important role in disk kinematics. In this project, our goal is to perform an orbital study of the stars in the inner disk and to show how these orbits are perturbed by the existence of the galactic bar.

The central bar-shaped structure is composed of stars in motion, and it is now understood that a bar is basically caused by regular orbits trapped around the so-called "x1" periodic orbits, these periodic orbits are our target. We use the same nomenclature used at [13]. Such orbital study with real data requires having the full 6D information for a sample of stars, i.e. coordinates, distance, proper motions and line-of-sight velocities. Test particle and N-body simulations have shed some light in the dynamics of inner disks, and only very recently we can use real data, with the combination of the astrometric Gaia (ESA) and spectroscopic surveys (e.g. APOGEE, LAMOST).

Our main goal is to use a sample of unprecedented size and coverage, given by the cross-match between the APOGEE DR16 and Gaia DR2 data, and classify the orbits into the different orbital families using computational techniques which allow us to work with large data sets.

To do so, we perform the following steps: we clean our data set and make an analysis of the most representative bulge-bar star population (Section II A). The cross-match between APOGEE DR16 and Gaia DR2 gives us data in the equatorial ICRS coordinate system, which we transform to the galactocentric coordinate system (Section II B). Once we have our sample expressed in the galactocentric coordinate system, we integrate the stars initial conditions to obtain the orbit (Section II C). With the orbit integrated for several revolutions, we run a Fourier transformation to obtain the frequencies and being able to separate the main bar orbital family from the main disk stars (Section III). With the resonances classified into the different bifurcations of the "x1" family, in Section IV, the project also wants to show evidence of how bar resonances give rise to distinct chemical signatures, and we compare it with recent studies. We finally expose our conclusions in Section V.

II. DATA AND TOOLS

A. Data

To get our data frame, in order to properly study the bar structure and the role that it plays in galaxies, we use the recent APOGEE DR16, the sixteenth data release (DR16) from the Sloan Digital Sky Surveys. This is the first time we also get data from the southern hemisphere giving us access to all major components of the Milky Way. DR16 also include data from previous releases [1]. To get the data we access the SDSS (Sloan Digital Sky Survey) Science Archive Server (SAS, https://data.ssds.org/sas/). APOGEE is performing a chemo-dynamical investigation across the entire galaxy providing us data and information about radial velocities, atmospheric parameters, and individual element abundances. We make use of the cross-match between Gaia DR2 and APOGEE already available in SAS. Our final data set contains a full 6D space coordinates (positions, proper motions and radial velocities) plus photometric information for 473.307 stars. With that information, we cut our sample to focus our project only to the inner disk, so we keep the information of the stars within $\mid b \mid < 25^o$ and $-25^o < l < 40^o$, where b and l are the galactic latitude and longitude. This results in a sample of 92499 stars. From this sample we use the following strategy to select the Red Clump (RC) stars, which are good standard candles for estimating astronomical distances:

1. For each star with galactic coordinates (l,b), we compute the extinction curve using the Drimmel extinction model [5]. We compute ((J-K),K) for $r \in [0, 12]$ kpc using 1000 bins, so a resolution

of $\sim 10\,\mathrm{pc}$, by assuming that the absolute magnitude in the K band of a Red Clump star is $M_K = -1.61\,\mathrm{mag}$ and with an intrinsic colour of $(J-K)_0 = 0.55\,\mathrm{mag}$ [3].

2. A star is a Red Clump star if $|((J-K) - (J-K)_{curve})| < 0.1$ mag, and we keep the heliocentric distance, d, when this occurs as the photometric distance of the star.

Using this strategy, we get a sub-sample of 12286 Red Clump stars with photometric distances.

Finally, in order to remove foreground stars and reaching the inner disk, we keep stars with heliocentric distance $d > 3$ kpc and $|v_x|, |v_y|$ and $|v_z| < 600$ km s^{-1}. Thus, the final sample consists of 9309 inner disc Red Clump stars.

B. Coordinate System

In this brief section, we explain the parameters we choose to change from the equatorial heliocentric coordinate system (ICRS) to the galactocentric, using the python library Astropy [15]. With a simple python code we change our coordinate system, firstly, from the ICRS to galactic heliocentric coordinates, and then from the galactic to the cartesian galactocentric coordinate. To change form the galactic frame to the galactocentric one, the position of the Sun is assumed to be on the x negative axis on the final, right-handed system, $R_\odot = 8.249$ kpc, $(U, V + V_{rot}, W) = (9.5, 250.7, 8.56)$ km s^{-1}[6].

Doing that, we obtain a 6D cartesian vector, (x, y, z, v_x, v_y, v_z), giving us the galactocentric positions and velocities, and we are ready to start analysing the dynamics of our sample.

C. Integration and Orbits

In order to perform the orbital analysis, we need to fix the Galactic potential. The model is a superposition of an axisymmetric component plus a bar potential. The axisymmetric component and rotation curve is from [2]. The bar model is an important topic which is treated in different publications, however, we will follow the model explained in [11], where the Galactic bar is modelled as a bar with a boxy/bulge with $M_{bar} = 10^{10} M_\odot$, $\Omega_p = 50$ km s^{-1} kpc^{-1}, $a = 4.5$ kpc, where M_{bar} is the mass of the bar, Ω_p is its pattern speed and a is the total length of the semi-major axis of the bar. We use the rest of parameters that are also exposed in [11].

All the model information of the bar potential in which we will run the integration is included in a Fortran 77 program that follows the algorithm for a Runge-Kutta method to resolve the differential equations that our chosen model present and that we run for each one of the particles of our final sample.

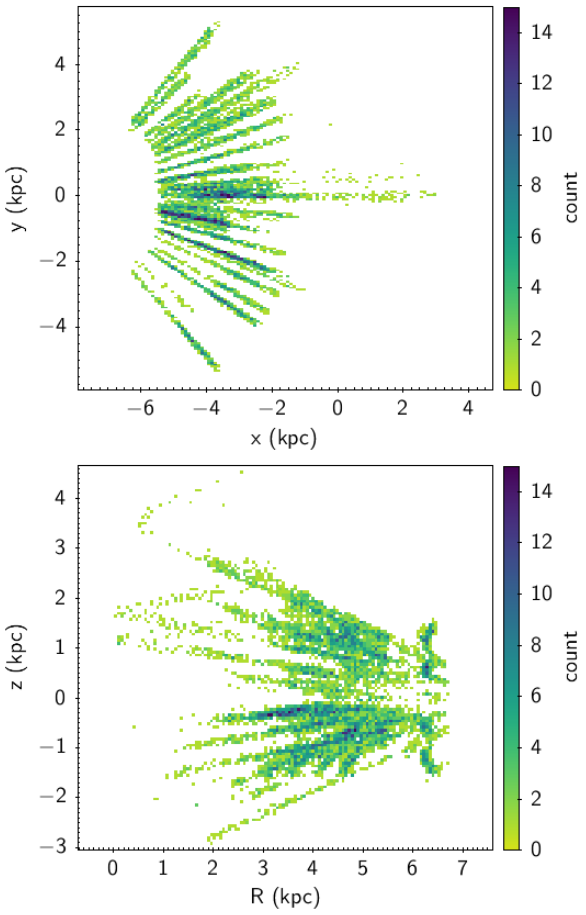

FIG. 1: Galactocentric (x, y) (top) and (R, z) (bottom) projections of the final sample.

The resulting outputs of running this code are two different files containing the spatial trajectories followed by all the studied objects in two different frames, an inertial one and a no-inertial one. In both frames, the center of the mass of the model is located at the origin. In the inertial frame, an observer sees the bar inclined respect to the (x, y) Galactic plane, and rotating along the z axis with constant angular velocity. In the no-inertial frame, an observer would rotate with the bar at the same constant velocity. To perform the frequency analysis (see Section III), we only take the information we get from the file that saves the trajectories in the no-inertial frame, where the whole system follows the movement of the bar.

We now have information about the dynamical evolution of all the studied stars and we are ready to do a frequency analysis to classify the orbits into the different orbital families. The Galactic bar model is known to have five different Lagrangian points, L_1 and L_2 are on the x-axis, L_3 in the origin of coordinates and L_4 and L_5 on the y-axis. The main family of periodic orbits is known as "x1" [13] and it provides the building blocks of the Galactic bar. Inside this family, most of the orbits have radial resonances 1:2, 1:3 and 1:4. In the top panels of

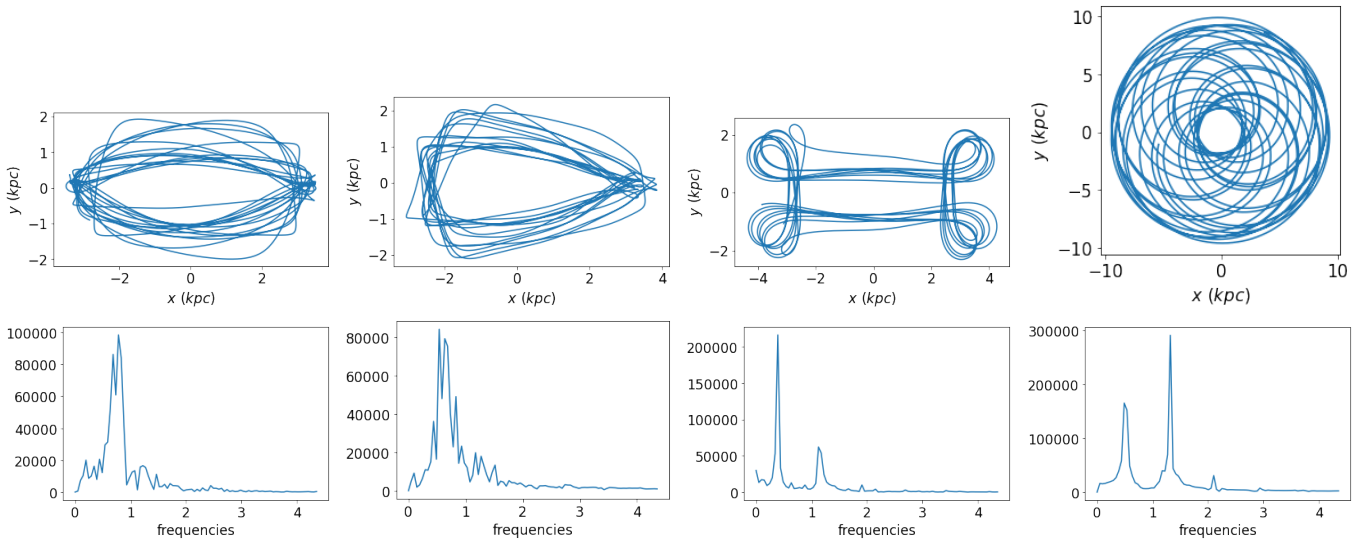

FIG. 2: (x, y) projection of orbits and their frequency histograms. We present the orbit (top) and the frequency histogram (bottom) of one star from each resonance. The order is: resonance 1:2 in the first column, resonance 1:3 in the second one, resonance 1:4 in the third one and disk at the fourth one.

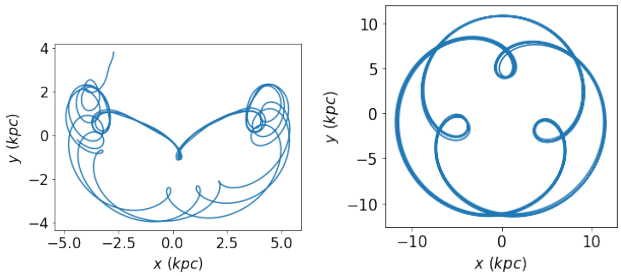

FIG. 3: XY projection of other bar-type orbits.

Fig. 2, we show the (x, y) projection of four typical orbits of our sample of stars. From left to right, orbits in 1:2, 1:3, 1:4 and disk. Besides the orbits related with the family "x1", that will be studied deeper in the next Section, we find stars belonging to the "x2" and "x3" families. Two examples of such orbits are plotted in Fig. 3. In the left panel, there is an orbit of manifold-type, this is, orbits orbiting from the L_1 towards the L_2 Lagrangian points, and viceversa, which are thought to be the the origin of the rR_1 rings of the [12]. In the right panel, we show a higher order resonant orbit, in particular, this is a 2:3 resonant orbit, this is, it makes two loops around the galactic centre, while it makes three radial loops.

III. KINEMATIC – FREQUENCY ANALYSIS

In this section we pay closer attention to the most important type of orbits when we talk about the bar structure, the "x1" family, and we group "x2" and "x3" families with the other no-bar families. We focus on quasi-periodic orbits elongated parallel to the bar, and classify the "x1" family into its bifurcations, 1:2, 1:3 and 1:4 resonance regions. In many cases, no suitable orbits beyond the 1:4 resonance can be found so we cut our study here.

From our final sample of stars and with each trajectory integrated we now proceed to do a frequency analysis of all of them. We want to extract the stars with typical bar motion (family "x1") and separate these into different files depending on its resonances. To do so we use Python once again, using a loop to open the dynamical information of each star: $(t, x, y, z, v_x, v_y, v_z)$. With that, and also using the same loop, we apply a Discrete Fourier Transform (DFT) to all of the orbits, using the FTT implementation from the numpy package of Python [16]. In order to establish a classification criterion, we seek patterns in the frequency-amplitude histogram for a smaller random subset of 306 stars. We focus on the frequency value of the most significant peak (freq). We, then, apply the adopted criteria to the full sample. The criteria we use is:

1. A star is classified as belonging to the 1:2 resonance if: $freq \in (0.78, 0.8)$.
2. A star is classified as belonging to the 1:3 resonance if: $freq \in (0.53, 0.54)$.
3. A star is classified as belonging to the 1:4 resonance if: $freq \in (0.39, 0.4)$.
4. The initial conditions of a star are classified into a file that contains no-bar stars if it has a number of peaks lower than six. We identified those stars with stars that have a high radial velocity and are able to escape the galaxy, that can happen because when we restricted the radial velocity of our sample we used a velocity higher than the escape velocity of the galaxy.

5. The initial conditions of a star are classified into a file containing all types of orbits if non of the previous requirements are accomplished.

Using this criteria, and focusing on the files containing the stars with typical bar motion, we obtain three files of different sizes, 42 stars for the 1:2 resonance, 137 stars for the 1:3 resonance and 99 stars for the 1:4 resonance. In the bottom panels of Fig. 2, we show the frequency histogram of the corresponding orbits in the top panel. We can appreciate the differences between different resonances. The star in the 1:4 resonance has, clearly, four radial excursions for each galactic period, while stars in the 1:3 resonance have three and stars in the 1:2 resonance have two. We can also note the difference between their frequency histograms, specially the second peak in the disk star histogram. Analyzing the classification, we notice that some typical disk orbits passed through the filter we used. The percentage of those disk-like orbits we get for each resonance is 2.33%, 27.01% and 51.52%, for the 1:2, 1:3 and 1:4 resonances, respectively. The total contamination of our files is a total of 31.90%. To improve this, we can notice that the no-bar orbits that passed through our filter have a second significant peak (p_2) in the frequency-amplitude phase space, compared to the most significant one (p_1). While the typical disk orbits have a significant second peak, this does not happen with the typical bar orbits. Imposing $p_1 > 2p_2$ we could reduce this elevated percentage of contamination. Note the difference between the frequency histograms of each family in Figure 3, specially the second peak of the disk-like orbit.

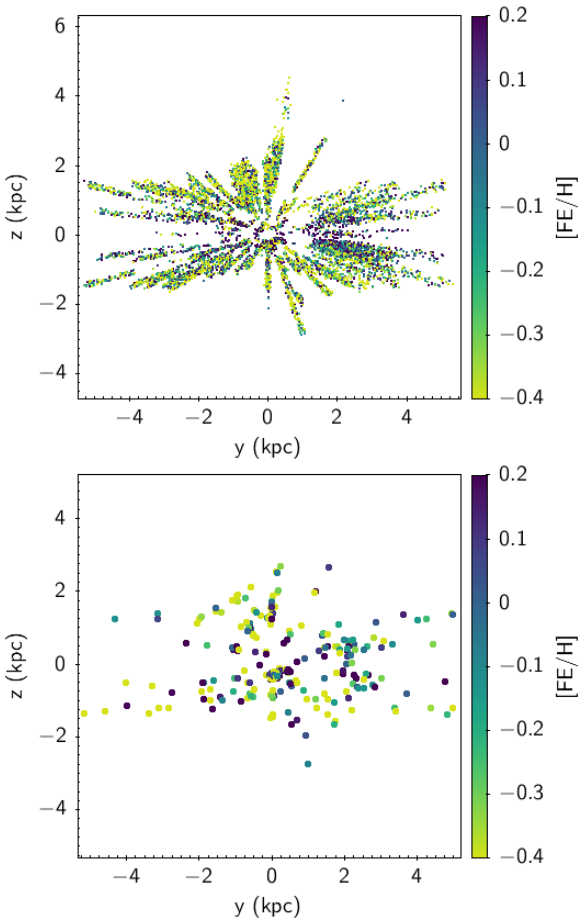

FIG. 4: (y, z) projection of our sample coloured with the [FE/H] abundance. The top figure is the sample with all the studied stars and the bottom one are the stars with typical bar motion.

IV. CHEMICAL ANALYSIS

The chemical composition of the bulge-bar region is complex. In this section we focus on the main chemical characteristics of our inner Galactic sample, which we had to filter once again to include sources with valid metallicities. Our data set has now a size of 8289 stars, with 250 stars with typical bar motion. We use the value [Fe/H] as representative of metallicity. We plan to study the effect of bar resonances on the inner Milky Way metallicity distribution.

Figure 4 shows the spatial chemical abundance for our sample, we plot the (y, z) Cartesian Galactic projection because, as it is seen in [14], the strongest signature is found at an azimuth along the bar's minor axis, while the resonant signature in the metallicity along the bar's semi-major axis almost vanishes. Analyzing Fig. 4, we confirm the vertical metallicity gradient, but we can not really appreciate any radial metallicity abundance gradient [8]. If we compute the median [Fe/H] abundance, though, we can find a small difference, suggesting the existence of a metal-poor component that seems to dominate the inner most part of our sample. We computed the following medians for all the sample, the bar stars and the 1:2 resonance, which is the resonance with less disk-like orbits stars contamination:

1. For the whole sample we have a [Fe/H] median abundance of -0.21947.
2. For stars with typical bar motion we have a [Fe/H] median abundance of -0.23427.
3. For the 1:2 resonance we have a [Fe/H] median abundance of -0.37594.

Figure 4 shows large metallicity values very close to $z \sim 0$, a result already known from previous studies [e.g., 1, 8]. But the projection also shows a considerable lack of data due to the APOGEE footprint, and we are not able to confirm if in the innermost part of the Milky way there is a metal-rich or a metal-poor star domination. There has been many similar studies trying to find a relationship between the metallicity of the stars and its birth place [e.g., 8, 9, 14], and their results do not all converge to the same conclusion. Here, if we take a close look to Fig. 4 top panel, we could think that the Milky Way has

a metal-rich bar population, but also doing an statistical analysis we find that bar resonance are composed by metal-poor stars. This property is still under research, and we have hit the same controversy that we find while reading different articles involved in the research, where each one of them provides a different result.

V. CONCLUSIONS

Using data from the cross-match between Gaia DR2 and APOGEE DR16, we classify stars with typical bar motion into different resonance types, one of our project objectives. To do that we first clean our sample and keep the significant stars of the inner galactic disk, then we change the coordinate system of our sample to the Cartesian galactocentric to be able to compute the trajectories of each star in the sample. With the dynamics, we make a frequency analysis and look for patterns in the frequency histograms of our sampled stars. We noticed three different patterns, each one followed by each resonant family and we are able to classify stars from these families. With the obtained results we compute the percentage of stars with disk-like orbits that passed through our filter, we also give a solution to reduce this contamination.

Another goal was to identify if there are chemodynamical signatures introduced by bar resonances in the Galactic disk, and we do not notice it projecting our data on the (y, z) Cartesian Galactocentric plane. But doing an statistical analysis of the [Fe/H] abundance of our data, we find the stars with typical bar motion are less rich in metallicity than stars classified into the global file containing stars with diverse orbital frequencies. However, the lack of data prevents us from stating whether the Galactic bar population is dominated by metal-rich stars or by metal-poor stars. This project can be improved in the near future by using more and with better accuracy data from future spectroscopic surveys (e.g. WEAVE@ING or 4MOST@VISTA).

Acknowledgments

To put an end to this project, I would really like to thank my supervisor Dra. Mercè Romero-Gómez for her guidance and for being always very helpful. I also want to thank my friends and colleagues, specially i would like to thank Robert Prat, who has helped me with the writing part. And finally I want to thank my family for being always there for me, specially my mother Isabel, my father Santiago and my twin brother Guillem.

[1] Ahumada, R.; Allende, C.; Almeida, A.; et al.; "The 16th Data Release of the Sloan Digital Sky Surveys: First Release from the APOGEE-2 Southern Survey and Full Release of eBOSS Spectra". The Astrophysical Journal Supplement Series, **249**: 1-21 (2020).

[2] Allen, C.; Santillán, K.; "An improved model of the Galactic mass distribution for orbit computations". Rev. Mexicana Astron. Astrof., **22**: 255-263 (1991).

[3] Alves; David, R.; "K-band calibration of the Red Clump luminosity". The Astrophysical Journal, **539**: 732-741 (2000).

[4] Antoja, T.; Helmi, A.; Romero-Gómez, M.; et al.; "A dynamically young and perturbed Milky Way disk". Nature , **561**: 360-362 (2018).

[5] Drimmel, R.; Cabrera-Lavers, A.; López-Corredoira, M.; "A three-dimensional Galactic extinction model", A&A, **409**: 205-215 (2003).

[6] Gravity coll.; Abuter, R.; Amorim, A.; "Detection of the Schwarzschild precession in the orbit of the star S2 near the Galactic centre massive black hole", A&A, **636**: 1-14 (2020).

[7] Helmi, A.; Babusiaux, C.; Koppelman, H.H.; et al.; "The merger that led to the formation of the Milky Way's inner stellar halo and thick disk". Nature, **563**: 85-88 (2018).

[8] Queiroz, A.; Chiappini, C. ; Perez-Villegas, A.; et al.; "The Milky Way's bar and bulge revealed by APOGEE DR16 and Gaia DR2", https://arXiv:2007.12915: 1-24 (2020)

[9] Rojas-Arriagada, A.; Zasowski, G.; Schultheis, M.; et al.; "How Many Components? Quantifying the Complexity of the Metallicity Distribution in the Milky Way Bulge with APOGEE". Monthly Noticies of the Royal Astronomiacl Society, **000**: 1-20 (2020).

[10] Romero-Gómez, M.; Mateu, C; Aguilar, L.; et al.; "Gaia kinematics reveal a complex lopsided and twisted Galactic disc warp", A&A, **625**: 1-25 (2019).

[11] Romero-Gómez, M.; Figueras, F.; Antoja, T.; et al.; "The analysis of realistic stellar Gaia mock catalogues - I. Red clump stars as tracers of the central bar", Monthly Notices of the Royal Astronomical Society, **447**: 218-233 (2015).

[12] Romero-Gómez, M.; Masdemont, J.J.; Athanassoula, E.; et al.; "The origin of rR1 ring structures in barred galaxies", A&A, **453**: 39-45 (2006).

[13] Skokos, Ch.; Patsis, P.A.; Athanassoula, E.; "Orbital dynamics of three-dimensional bars – I. The backbone of three-dimensional bars. A fiducial case", Mon. Not. R. Astron. Soc., **333**: 847-860 (2002).

[14] Wheeler, A.; Abril-Cabezas, I.; Trick, W.H.; et at.; "Chemodynamical signatures of bar resonances in the Galactic disk: current data and future prospects", https://arxiv.org/abs/2105.05263: 1-15 (2021).

[15] https://docs.astropy.org/en/stable/coordinates/

[16] https://numpy.org/doc/stable/reference/routines.fft.html